

Urban Heat Island Amplification Estimates on Global Warming Using an Albedo Model

Alec Feinberg

Key Words: Urban Heat Islands, Albedo Modeling, UHI Amplification Effects, Global Warming Causes and Amplification Effects, UHI Footprint, UHI Heat Dome, Cool Roofs, Sea Ice and Moisture Feedbacks

Abstract In this paper we provide nominal and worst case estimates of radiative forcing due to UHI effect (including urban areas) using a Weighted Amplification Albedo Solar Urbanization (WAASU) Model. This is done with the aid of reported findings from UHI footprint and heat dome studies that simplified estimates for UHI amplification factors. Using this method, we find between 1.2 and 15% of global warming may be due to the UHI effect (with urban areas). These values may increase in terms of the root-cause assessment to 2.9 and 27% when climate feedback values are estimated. These large variations are due to urbanized area and UHI area amplification factor uncertainties. However, the model showed consistent estimates of about $0.096(\text{W}/\text{m}^2)/(\%\text{Effective Normalized Area})$ for the urbanized area feedback value. The model is additionally used to quantify an assessment of sea ice feedback warming. Results provide insight into the UHI area effects from a new perspective and illustrates that one needs to take into account effective UHI amplification factors when assessing UHI's warming effect on a global scale. Lastly, such effects likely show a persuasive argument for the need of world-wide UHI albedo goals.

1 Introduction

It is concerning that there are so few UHI publications recently on their possible influences to global warming. Part of the motivation for this paper is to illustrate the continual need for more up-to-date related studies including UHI amplification effects (that include their urban areas) as will be discussed in this paper. The subject of UHI effect having significant contributions to global warming is very important and should remain so. The topic has a controversial history. One such paper, McKittrick and Michaels (2007) found that the net warming bias at the global level may explain as much as half the observed land-based warming. This study was criticized by Schmidt (2009) and defended for a period of about 10 years by Mckittrick (see McKittrick Website). Other authors have also found significance (Zhao, 1991; Feddema et al., 2005; Ren et al., 2007, 2008; Jones et al., 2008; Stone, 2009; Zhao, 2011; Yang et al. 2011, and Haung et al. 2015). These studies used land-based temperature station data to make assessments. Although the studies have all found global warming UHI significance with different assessments, they have yet to influence the IPCC enough to necessitate albedo recommendations in their many reports and meetings like the CO₂ effort. This is important because we feel the IPCC's should be more proactive in helping the global community recognizing the need for UHI albedo guidelines. Although the IPCC have provided reports on UHIs including health related issues, the response to their reports does not appear to be effective on the global scale compared with the on-going CO₂ effort.

The contention that UHI effects are basically only of local significance is most likely related to urban area estimates. For example, IPCC (Satterthwaite et. al. 2014) AR5 report references Schneider et al. (2009) study that resulted in urban coverage of 0.148% of the Earth (Table 1). This seemingly small area tends to dismiss the contention that UHI effect can play a large scale role in global warming. Furthermore, estimates of how much of land has been urbanized vary widely in the literature and this is in part due to the definition of what is urban and the datasets used. Although, such estimates are important for environmental studies, obtaining true estimates for the small urbanized area relative to the total land is apparently very difficult. This is compounded by the fact that there is a significant difference in how groups define the term 'urban'. Thus, urbanized surface area land approximations vary widely and most are obtained with satellite measurements sometimes supplemented in some way with census data. Table 1 captures the variations from some papers that are of interest.

Table 1. Urbanization area extent estimates from various sources

Percent of Land	Percent of Earth	References
2.7	0.783	GRUMP, 2005 - using NASA satellite light studies based on 2004 data and supplemented with census data
1%	0.29	NASA, 2000; Galka, 2016 – from satellite data
0.51	0.148	Schneider et al. 2009 - based on 2000-2001 data and referenced in the IPCC report (Satterthwaite, 2014)
0.5%	0.145	Zhou 2015 - based on a 2000 data set

56 In addition, global warming UHI amplification effects have not been quantified to a large degree related to area
57 estimates. Urbanized average solar areas remain unknown.

58
59 In our study, one key paper listed in the Table 1 is due to Schneider et al. (2009) since it is cited by the AR5 2014
60 IPCC report (Satterthwaite et al. 2014). In Schneider's paper, the larger area found in the GRUMP 2005 study
61 (Table 1) is criticized. These area estimates are of interest in our paper for the *Weighted Amplification Albedo Solar*
62 *Urbanization (WAASU) Model*. As well, the Amplification factors we use are related to their urban coverage
63 estimates. In this paper we use both the Schneider et al. and GRUMP studies for the nominal and worst cases
64 urbanization area estimates respectively. Furthermore, they were both done using data sets from around 2000 which
65 is a convenient time to extrapolate down to 1950 and up to 2019 (see Sec. 3).

66
67 In our study, where we introduce the WAASU model, we will see that it has some advantages over the ground-based
68 temperature studies like McKittricks and Michaels. The model is non probabilistic, in line with the way typical
69 energy budgets are calculated. It uses only two key parameters (effective normalized area and average albedo).
70 Because it is simplistic, it has transparency compared with the complex land-based studies.

71 72 *1.1 UHI Amplification Effects*

73
74 The table below lists the global warming causes and amplification effects. In this section we will summarize only
75 the UHI amplification effects listed in the table since the root causes and the main global warming feedback
76 amplification effects are fairly well known.

77
78 **Table 2.** Global warming cause and effects

Global Warming Causes →	Population → Expanding Urban Heat Islands (UHI), Roads & Increases in Greenhouse Gas
Global Warming Feedback Amplification Effects →	Water Vapor Feedback, Land Albedo Change Due to Cities & Roads, Ice and Snow –Albedo Feedback, Lapse Rate Feedback, Cloud Feedback, etc.
Urban Heat Island Amplification Effects →	UHI Solar Heating Area (Building Areas), UHI Building Heat Capacities, Humidity Effects and Hydro-Hotspots, Reduced Wind Cooling, Solar Canyons, Loss of Wetlands, Increase in Impermeable Surfaces, Loss of Evapotranspiration Natural Cooling.

79
80 The UHI amplification effects that we consider to dominate listed in the table are as follows:

- 81
- 82 • ***The humidity amplification effect:*** This has been observed. For example, Zhao et al. (2014) noted that UHI
83 temperature increases in daytime ΔT by 3.0°C in humid climates but decreasing ΔT by 1.5°C in dry
84 climates. They noted that such relationships imply that UHIs will exacerbate heat wave stress on human
85 health in wet UHI climates. One explanation for this is how heat dissipates through convection which is
86 more difficult in humid climates. Another explanation is that warmer air holds more water vapor. This can
87 increase local specific humidity so that there could be local greenhouse effects.
 - 88
 - 89 • ***The heat capacity and solar heating area amplification effect:*** This contributes to the day-night UHI
90 cycle. Here in most cities, it is observed that daytime atmospheric temperatures are actually cooler
91 compared to night. For example, in a study by Basara et al. (2008) in Oklahoma city UHI it was found that
92 at just 9-m height, the UHI was consistently $0.5\text{--}1.75^{\circ}\text{C}$ greater in the urban core than the surrounding rural
93 locations at night. Further, in general UHI impact was strongest during the overnight hours and weakest
94 during the day. This inversion effect can be the results of massive UHI buildings acting like heat sinks,
95 having giant heat capacities and storing heat in their reservoir via convection as solar radiation is absorbed
96 during the day. This often reduces the UHI day effect, but at night buildings cool down, giving off their
97 stored heat that increases local temperatures to the surrounding atmosphere. This effect increases with city
98 growth as buildings have gotten substantially taller (Barr 2019) since 1950.
 - 99
 - 100 • ***The hydro-hotspot amplification effect:*** This effect is not well addressed. Here atmospheric moisture
101 source is a complex issue due to Hydro HotSpots (HHS). Hydro hotspots occur when buildings are hot due
102 to sun exposure. Then during precipitation periods, the hot highly evaporation surfaces increase localized
103 water vapor in the air via the effect that warm air holds more moisture. This increase in local greenhouse
104 gas, could blanket city heat and increase infrared radiation during these periods. This, as discussed above,
105 is another possible UHI humidity amplification.
 - 106
 - 107 • ***Reduced wind cooling and solar canyons:*** In UHIs reduced wind is a known effect due to building wind
108 friction which inhibits cooling by convection. As well, tall buildings create solar canyons and trap sunlight

109 reducing the average albedo although some benefits occurs from shading. In general, both have the effect
 110 of amplifying the temperature profile of UHIs.
 111

112 2 Data and Methods

113
 114 We see from the previous section that estimating climate change impact just based on the UHI and Urban area
 115 coverage as in Table 1, cannot take into account solar heating building sidewall areas, massive heat capacities, the
 116 humidity effects, wind reduction and the solar canyon effect which amplify UHI effects beyond its own climate area.

117 2.1 UHI Area Amplification Factor

118
 119 In order to estimate the UHI amplification effects, it is logical to first look at UHI footprint (FP) studies as they
 120 provide some measurement information. Zhang et al. (2004) found the ecological footprint of urban land cover
 121 extends beyond the perimeter of urban areas, and the footprint of urban climates on vegetation phenology they found
 122 was 2.4 times the size of the actual urban land cover. In a more recent study by Zhou et al. (2015), they looked at
 123 day-night cycles using temperature difference measurements. In this study they found UHI effect decayed
 124 exponentially toward rural areas for majority of the 32 Chinese cities. Their study was very thorough and extended
 125 over the period from 2003 to 2012. They describe China as an ideal area to study since it has experienced the
 126 rapidest urbanization in the world in the decade they evaluated. They found that the “footprint” of UHI effect,
 127 including urban areas, was 2.3 and 3.9 times of urban size for the day and night, respectively. We note that the
 128 average day-night amplification footprint coverage factor is 3.1.

129 Looking at Table 2, we see that the UHI Amplification Factor (AF) is highly complex making it difficult to assess
 130 from first principles as it would be some function of Table 2 components:

$$131 \quad AF_{UHI \text{ for } 2019} = f\left(\overline{Build}_{Area} \times \overline{Build}_{C_p} \times \overline{R}_{wind} \times \overline{LossE}_{vtr} \times \overline{Hy} \times \overline{S}_{canyon}\right) \quad (1)$$

132 were

133 \overline{Build}_{Area} = Average building solar area

134 \overline{Build}_{C_p} = Average building heat capacity

135 \overline{R}_{wind} = Average city wind resistance

136 \overline{LossE}_{vtr} = Average loss of evapotranspiration to natural cooling & loss of wetland

137 \overline{Hy} = Average humidity effect due to hydro-hotspot

138 \overline{S}_{canyon} = Average solar canyon effect

139

140 As a helpful example, one basic formulation that might be suggested is a product of power law average ratios over
 141 all urban cities compared to a reference year (1950) such that
 142

$$143 \quad AF_{UHI \text{ for } 2019} = \left(\frac{(\overline{Build}_{Area})_{2019}}{(\overline{Build}_{Area})_{1950}}\right)^{N_1} \left(\frac{(\overline{Build}_{C_p})_{2019}}{(\overline{Build}_{C_p})_{1950}}\right)^{N_2} \left(\frac{(\overline{R}_{wind})_{2019}}{(\overline{R}_{wind})_{1950}}\right)^{N_3} \left(\frac{(\overline{LossE}_{vtr})_{2019}}{(\overline{LossE}_{vtr})_{1950}}\right)^{N_4} \left(\frac{(\overline{Hy})_{2019}}{(\overline{Hy})_{1950}}\right)^{N_5} \left(\frac{(\overline{S}_{canyon})_{2019}}{(\overline{S}_{canyon})_{1950}}\right)^{N_6} \cdot (2)$$

144

145 In order to provide some estimate of this factor, we note that Zhou et al. (2015) found the FP physical area (km²),
 146 correlated tightly and positively with actual urban size having correlation coefficients higher than 79%. This
 147 correlation can be used to provide an initial estimate of this complex factor. Therefore, as a model assumption, it
 148 seems reasonable to use area ratios for this estimate. Area estimates have been obtained in the next Section in Table
 149 3 between 2019 and 1950 time frames. These yield the following results for the Schneider et al. (2009) and the
 150 GRUMP (2005) extrapolated area results:

$$151 \quad AF_{UHI \text{ for } 2019} = \frac{(Urban \text{ Size})_{2019}}{(Urban \text{ Size})_{1950}} \approx \begin{cases} \left(\frac{[0.188]_{2019}}{[0.059]_{1950}}\right)_{Schneider} = 3.19 \\ \left(\frac{[0.952]_{2019}}{[0.316]_{1950}}\right)_{GRUMP} = 3.0 \end{cases} \quad (3)$$

152 Between the two studies, the UHI area amplification factor average is 3.1. Coincidentally, this is the same factor
 153 observed in the Zhou et al. (2015) study for the average footprint. This factor may seem high. However, it is likely

154 conservative. There are other effects that would be difficult to assess. For example, increases in global draught due
 155 to loss of wet lands, deforestation effects due to urbanization and draught related fires. It could also be important to
 156 factor in changes of other impermeable surfaces since 1950 such as highways, large impermeable surfaces (parking
 157 lots and event centers), and so forth.

158
 159 The area amplification value of 3.1 is then considered as one of our model assumptions.
 160

161 **2.2 Alternate Method Using the UHI's Horizontal Extent**

162
 163 An alternate approach to check the estimate of Equation 3, is to look at the UHI's dome extent. Fan et al. (2017)
 164 using an energy balance model to obtain the maximum horizontal extent of a UHI heat dome in numerous urban
 165 areas found the nighttime extent of 1.5 to 3.5 times the diameter of the city's urban area (2.5 average) and the
 166 daytime value of 2.0 to 3.3 (2.65 average).

167
 168 Applying this energy method (instead of the area ratio factor in Eq. 3), yields a diameter in 2019 compared to that of
 169 1950 increase of about 1.8. This implies a factor of $2.5 \times 1.8 = 4.5$ higher in the night and $2.65 \times 1.8 = 4.8$ in the day in
 170 1950 (average 4.65). This increase occurs 62.5% of the time according to Fan et al., (where their steady state
 171 occurred about 4 hours after sunrise and about 5 hours after sunset) yielding an effective UHI amplification factor of
 172 2.9. We note this amplification factor is in good agreement with Equation 3. Fan et al. assessed the heat flux over the
 173 urban area extent to its neighboring rural area where the air is transported from the urban heat dome flow. Therefore
 174 the heat dome extends in a similar manner as observed in the footprint studies. If we use the dome concept, we can
 175 make an assumption that the actual surface area for the heat flux is increase by the surface area of the dome. We
 176 actually do not know the true diameter of the dome, but it is larger than the assessment by Fan et al.. Using the dome
 177 extend due to Fan et al. applied to the area of diameter D , the amplification factor should be correlated to the ratios
 178 of the dome surface areas as
 179

$$180 \quad AF_{UHI, for 2019} = \left(\frac{D_{2019}}{D_{1950}} \right)^2 = 2.9^2 = 8.4 \quad (4)$$

181 Thus, this is our second model assumption, where it is reasonable to use the ratios of the dome's surface area for an
 182 alternate approach in estimating the effective UHI amplification factor. In this way we will have two values, 3.1 and
 183 8.4 to work with which will help in assessing model consistency and provide upper and lower bounds for effective
 184 area amplification which must occur based on these authors observations and the dependence in Equation 1.
 185

186 **2.3 Applying the Amplification Factors**

187
 188 In this analysis, 1950 is the reference year. Therefore it is not subjected to amplification. Only the new area is
 189 amplified as we are looking at changes since this time frame. This is denoted as the Amplified Effected Area (AEA).
 190 The AEF in 2019 is then given by
 191

$$192 \quad AEA_{UHI, for 2019} = AF(newarea) + Area_{1950} = AF(Area_{2019} - Area_{1950}) + Area_{1950} \quad (5)$$

193 In this, if there were no change so that the $Area_{2019} = Area_{1950}$, the resulting area is just the original $Area_{1950}$. This
 194 result is applied to the new area in Table 3 below.
 195

196 **2.4 Area Extrapolations for 1950 and 2019**

197
 198 In order to assess the urbanized area, (also used in determining the UHI amplification factor ratios above), we need
 199 to project the Schneider and GRUMP area estimates down to 1950 and up to 2019. Both use datasets from around
 200 2000 so this is a convenient somewhat middle time-frame. Here we decided to use the world population growth rate
 201 (World Bank 2018) which varies by year as shown in Appendix A in Figure A1. We used the average growth rate
 202 per ½ decade for iterative projections (about 1.3% to 1.6% per year).
 203

204 To justify this we see that Figure A2a illustrates that building material aggregates (USGS 1900-2006) used to build
 205 cities and roads correlates well to population growth (US Population Growth 1900-2006).
 206

207 It is also interesting to note that building materials for cities and roads also correlates well to global warming trends
 208 (NASA 1900-2006) shown in Figure A2b.

209
210
211
212
213
214

Column 2 in Table 3 show the projections with the actual year (~2000) data point tabulated value also listed in the table (also see Table 1). The UHI area amplification factor of 3.1 (Column 3) are then applied to Schneider and GRUMP studies shown in Column 4 using Equation 5.

Table 3. Extrapolated and amplified urbanized coverage estimates

Year	Urban coverage percent of Earth	Amplification factor effect	Amplification Effected Area (AEA)
Schneider study			
1950	0.059*	1	0.059%
2000-2001	0.0051x29%=0.148		
2019	0.188*	3.1 AF _{Area} **	0.459%
2019	0.188*	8.4 AF _{Dome} **	1.143%
Worst case GRUMP study			
1950	0.316%*	1	0.316%
2000	0.027x29%=0.783%		
2019	0.952%*	3.1 AF _{UHI} **	2.288%
2019	0.952%*	8.4 AF _{Dome} **	5.658%

*Growth rate of cities using world population yearly growth rate in Fig A1, **AF_{UHI} is the area amplification factor for 2019 referenced to 1950.

215
216
217

2.5 Weighted Amplification Albedo Solar Urbanization (WAASU) Model Overview

218
219
220
221

The WAASU model is very straightforward; it is based on a global weighted albedo model. The Earth Albedo is given by

$$Earth\ Albedo = \sum_i \{ \% Effective\ Surface\ Area_i \times Surface\ Item\ Albedo_i \} + Cloud\ Area \times Cloud\ Albedo. \quad (6)$$

222
223
224

Here the effective surface area is given by

$$Effective\ Surface\ Area = Surface\ Area \times \% Solar\ Irradiance. \quad (7)$$

225
226

where the surface area includes all areas including AEA. We note that the change in the Earth Albedo change over time (from 1950 to 2019), is just a function of the UHI area variation, (when holding all unrelated UHI components fixed), that is

229
230

$$\left(\frac{dEA}{dt} \right)_{EA'} = \sum \left(Albedo_{UHI} \times Solar\ Irradiance \times \frac{dArea_{UHI}}{dt} \right)_i, \quad (8)$$

231

232

where EA is the Earth Albedo, and EA' are all other Earth components (held fixed). Although it is possible that the solar irradiance percent changes due to new city locations, in this model we assume it is fixed at 100%. This indicates, for example, that even if we were to change the *Effective Surface Area* of perhaps the *sea ice component* due to the fact that it receives about 40% irradiance compared with other areas and redistributed its radiance (per the Earth's energy budget), it would not affect the overall results when looking at the albedo change due to the UHI effect from 1950 to 2019. Therefore, the model allows freedom to only work with normalized area coverage changes when focusing on the UHI effect. On the other hand, solar irradiance comes into play for sea ice when we are considering its global albedo effect from 1950 to 2019 (see Appendix C). However, the solar radiation weighting, albedo, and areas for all Earth components are subjected to the constraints below.

242

2.5.1 Model Constraints

243
244

This model is subject to the constraint

245
246

$$Total\ Area = \sum_i \{ \% Earth\ Surface\ Areas_i \} + \% Cloud\ Area = 100\% \quad (9)$$

247
 248 and the normalization constraint for the Earth surface areas (when the UHI area is increased) must then be subject to
 249

$$250 \quad \sum_i \{\% \text{Earth Surface Areas}_i\} = 100\% - \% \text{Cloud Area}. \quad (10)$$

251
 252 To simplify things as much as possible, only five Earth constituents are used: *water, sea ice, land, UHI coverage,*
 253 *and clouds* (where *land* is its area minus the UHI coverage). These components are fairly easy to estimate and
 254 references for their values are provided in Appendix D. Furthermore, we use consistent values found in the IPCC
 255 AR5 report (Hartmann et al., 2013) assessment of the Earth’s energy budget for solar irradiance. Table 4
 256 summarizes the constraints from these IPCC values.

257
 258 The fixed components of our model maintain relative consistency from 1950 to 2019. The non-fixed value is the
 259 urban coverage as indicated by Equation 8. The only unknown value is the *land* albedo (minus the UHI coverage)
 260 and this value is adjusted to obtain the IPCC global albedo of 29.4118% and its *land* value of incident/reflected
 261 value of 7.0588.

262 **Table 4. IPCC Earth energy budget values (Hartmann et al., 2013)**

IPCC Item	Incident and Reflected Radiation (W/m ²)	Albedo %	Absorbed (W/m ²)
Earth	100/340	29.4118	240=340x(1-.294)
Atmosphere & Clouds	76/340	22.3529	79
Earth Surface Albedo	24/340	7.0588	161

263
 264 These values are used as a 1950 starting point and then the 2019 increase for UHI coverage area is inserted. This
 265 increases the Earth’s area to greater than 100%. Therefore, renormalization is done per the constraint of Equation 10
 266 (detailed in Appendix B).

267
 268 **3 Results and discussion**

269
 270 Using the extrapolated area coverage in Table 3 with the 3.1 amplification factor applied to the urbanized growth,
 271 the resulting global albedo change occurred of 29.3956% in 2019 (Table 5b) compared to the earlier 1950 albedo
 272 value of 29.4118% (Table 5a) for the Schneider nominal case. As well, for the GRUMP worst case, the albedo
 273 changed from 29.4118% (Table 6a) to 29.3322% (Table 6b) due to the urbanized growth.

274
 275 As we mentioned earlier, the increases in the solar surface area of the Earth, which will occur with city growth of
 276 tall buildings and their solar areas, however comparatively small, requires renormalization in the model of the Earth
 277 surface components of the WAASU model (detailed in Appendix B). This is displayed in column 3 in Tables 5b and
 278 6b. While the model is sensitive to urban coverage changes, it works well with renormalization showing a high level
 279 of consistency to urban coverage proportionality changes. This is indicated in Table 7 where we find the GRUMP
 280 2019 area feedback is 0.0944% (W/m²)/Norm Area (=0.271/2.87) compared with the Schneider area feedback of
 281 0.0948 (W/m²)/ %Norm Area (=0.055/0.58).

282
 283 Table 7 provides a summary of albedo changes found in the WASSU model along with the expected solar long wave
 284 radiation increase. From the above global WAASU model, the estimates of the Earth’s radiated long wavelength
 285 emissions are set equal to the short wave radiation absorption:

$$286 \quad P_{\text{Total}} = 340 \text{ W/m}^2 (1 - \text{Albedo}). \quad (11)$$

287
 288
 289 Then the change from 1950 to 2019 represents the equivalent increase in long wave radiation is given by

$$290 \quad \Delta P_{\text{Total}} = 340 \text{ W/m}^2 \{(1 - \text{Albedo})_{2019} - (1 - \text{Albedo})_{1950}\}. \quad (12)$$

298 **Table 5a.** Schneider results (Albedo=29.4118, 1950) **Table 5b.** Schneider results (Albedo=29.3956%, 2019)

Surface	Albedo		Normalized Weighted	
	A	B	C=A x B x (1-0.67)	A x C
Sum of Water Type		71		
Sea Ice	0.6	15	4.95	2.970
Water	0.06	56	18.48	1.109
Sum of Land Type		29		
Land - (UHI + Coverage)	0.3118	28.941	9.55053	2.978
UHI + Coverage	0.12	0.059	0.01947	0.002
		Σ=100.000	33.000	7.05882
			Cloud Area	
Clouds	0.3336	67	67	22.35294
Σ Sum Earth %			100.000	
Σ Global Albedo				29.4118

Surface	Albedo		Normalized Weighted	
	A	B	C=A x B x (1-0.67)	A x C
Sum of Water Type		70.717		
Sea Ice	0.6	14.94	4.9302	2.958
Water	0.06	55.777	18.406	1.1044
Sum of Land Type		29.283		
Land - (UHI + Coverage)	0.3118	28.826	9.513	2.966
UHI + Coverage	0.12	0.4571	0.1508	0.0181
		Σ=100.000	33.000	7.0283
			Cloud Area	
Clouds	0.3336	67	67	22.3530
Σ Sum Earth %			100.000	
Σ Global Albedo				29.3994

299

300 **Table 6a.** GRUMP results (Albedo=29.4118, 1950) **Table 6b.** GRUMP results (Albedo=29.3322%, 2019)

Surface	Albedo		Normalized Weighted	
	A	B	C=A x B x (1-0.67)	A x C
Sum of Water Type		71		
Sea Ice	0.6	15	4.95	2.970
Water	0.06	56	18.48	1.109
Sum of Land Type		29		
Land - (UHI + Coverage)	0.3135	28.684	9.46572	2.968
UHI + Coverage	0.12	0.316	0.10428	0.013
Sum Surface %		Σ=100.000	33.000	7.0588
			Cloud Area	
Clouds	0.3336	67	67	22.3529
Σ Sum Earth %			100.000	
Σ Global Albedo				29.4118

Surface	Albedo		Normalized Weighted	
	A	B	C=A x B x (1-0.67)	A x C
Sum of Water Type		69.627		
Sea Ice	0.6	14.71	4.8543	2.913
Water	0.06	54.917	18.12261	1.087
Sum of Land Type		30.3727		
Land - (UHI + Coverage)	0.3135	28.129	9.28257	2.910
UHI + Coverage	0.12	2.2437	0.740421	0.089
Sum Earth %		Σ=100.000	33.000	6.9100
			Cloud Area	
Clouds	0.3336	67	67	22.3530
Σ Sum Earth %			100.000	
Σ Global Albedo				29.3519

301

302 Results are compiled in Table 7. The table also includes “what if” estimates, if we could change urbanization to be
 303 more reflective with cool roofs to reverse the effect.

304

305 The general results are summarized:

- 306 • Nominal Schneider case from 1950 to 2019 is 0.042 and 0.113 W/m² due to urban area and dome
 307 amplification coverage respectively. These would equate to about 1.18% and 3.2% of global warming
 308 assuming the total increase from 1950 is about 0.95°C in 2019.
- 309 • Worst GRUMP case from 1950 to 2019 is 0.204 and 0.537 W/m² due to urban area and dome amplification
 310 coverage respectively. This would roughly equate to about 5.7 and 15% of global warming assuming the
 311 total increase from 1950 is about 0.95°C in 2019.
- 312 • We note the consistency of the area feedback parameter having quite small variability and averaging about
 313 0.096 W/m²/Effected %Normalized Area
- 314 • “What if” corrective action results of cool roofs indicates that changing city albedos in both the Schneider
 315 and the GRUMP case from 0.12 to an average value of 0.205 would reverse the increase in emission back
 316 to 1950 levels.

317

318 Although global warming assessment obtained in the WAASU model, especially for the Schneider case does not
 319 appear to show much contribution to global warming, we find that climate feedback estimates increase the estimated
 320 root-cause proportion significantly. Examples are provide in Appendix C that help to demonstrate how the root-
 321 cause global warming contribution can be as go as high as 7.3% for the Schneider case and 27% for the GRUMP
 322 case (see Table C2).

323

324

325

326

327

328
329

Table 7. Albedo and radiative increase model results with UHI effective area.

Year	Urban Extent Global Area %	UHI Effective Global Surface % Area	UHI Effective Normalized Global Surface %Area	Albedo Cities	Global Weighted Albedo	ΔP_{Total} UHI Radiative Increase W/m^2 (%GW)*	Area Feedback $\frac{\Delta P_{Total} (W/m^2)}{Ef Norm \% Area}$
Nominal Case Schneider Study							
1950	0.059	0.059	0.059	0.12	29.4118	0	—
2019	0.188	0.459 (Area AF)	0.457	0.12	29.3994	0.0422 (1.18%)*	0.092
2019	0.188	1.143 (Dome AF)	1.1307	0.12	29.3786	0.1129 (3.16%)*	0.1
What if	0.188	0.459, 1.58 (Area-Dome AF)	0.457, 1.13	0.202, 0.209	29.4118	-0.042-0.113 (-1.18, -3.16%)*	—
Worst Case GRUMP Study							
1950	0.316%	0.316	0.316	0.12	29.4118	0	—
2019	0.952%	2.288 (Area AF)	2.2437	0.12	29.3519	0.204 (5.7%)*	0.091
2019	0.952%	5.658 (Dome AF)	5.395	0.12	29.2539	0.537 (15%)*	0.1
What if	0.952%	2.288, 5.658	2.2437, 5.395	0.2009, 0.2087	29.4118	-0.204(-5.7%)* -0.537(-15%)*	—

*Percent of Warming estimate, $P=340 \times (1-\text{Albedo})$, $\%GW=\{(P/\epsilon\sigma)^{0.25}_{2019}- (P/\epsilon\sigma)^{0.25}_{1950}\}/0.95^\circ C$, $\epsilon=1$

330
331
332
333

4 Conclusions

334
335
336
337
338
339
340
341
342
343
344
345

In this paper we were able to provide estimates of UHI effect (with urban area) on global warming. This was done with the aid of assumptions for area UHI amplification factors. These estimates inserted into our WAASU model found that between 0.042 and 0.537 W/m² of radiative forcing is possible according the WAASU model (this results indicates that about 1.2 and 15% of global warming may be due to the UHI effect (with urban areas). This wide variation is due to both the amplification and urban area uncertainties. However, the model found that the effective UHI area feedback estimates were consistent and about 0.096(W/m²)/(%Effective Normalized Area). Examples are provided in Appendix C to illustrate how the UHI root-cause assessment to global warming increases significantly when all climate feedback factor contributions are considered. The strength of the model is also demonstrated in Appendix C as estimates were obtained for global warming to the loss of sea ice in the last two decades. As area estimates and UHI amplification factors are very sensitive to the final results, it is clear refined values of both would be important for further study.

346

Below we provide suggestions and corrective actions which include:

347
348
349
350
351
352
353

- IPCC be more proactive in helping to providing albedo guidelines or recommendation similar to their CO₂ effort for both UHIs and roads.
- A guideline for future albedo design requirements of city and roads should be developed.
- Recommend an agency like NASA be tasked with finding applicable solutions to cool down UHIs.
- Recommendation for cars to be more reflective. Here although world-wide cars likely do not embody much of the Earth’s area, recommending that all new manufactured cars be higher in reflectivity (e.g., silver or white) would help raise awareness of this issue similar to electric cars that help improve CO₂ emissions.

354

355

Appendix A: Growth Rates and Information on Natural Aggregates

356
357
358
359
360

Below is a plot of the world population growth rate that varies from about 2.1 to 1.1. This is used to make growth rate estimates of urban coverage. We note that natural aggregate used to build cities and roads are reasonably correlated to population growth in Figure A2a. Also of interest (Fig. A2b) is the fact that one can see some correlation to global warming with the use of natural aggregates.

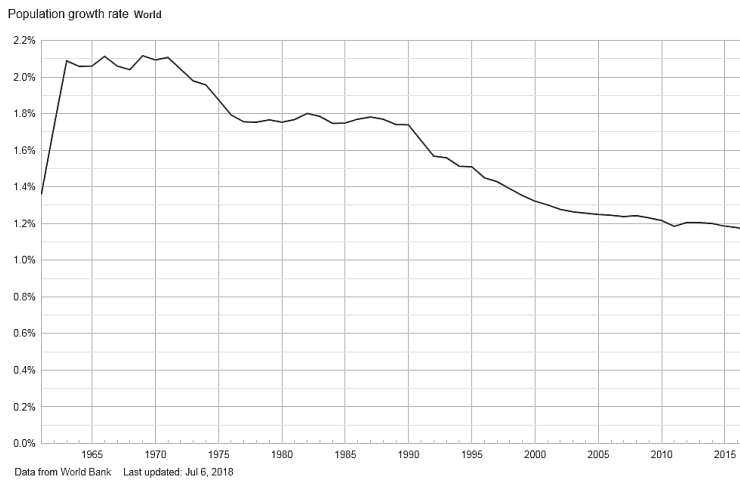


Figure A1. Population growth rate by year from 1960 to 2018, World Bank, 2018

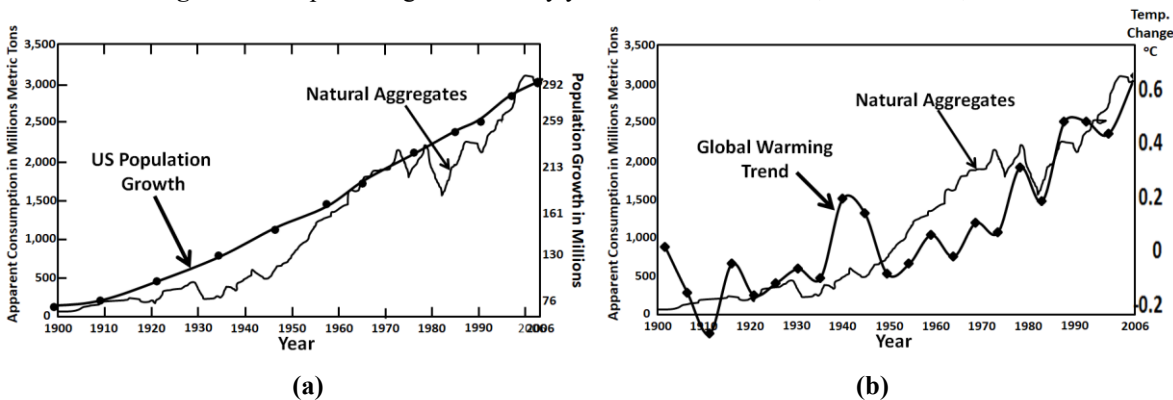


Figure A2. a) Natural aggregates correlated to U.S. Population Growth (USGS 1900-2006) b) Natural aggregates correlated to global warming (NASA 2020)

Appendix B: Albedo Model Normalization Information

Table 5a is reproduced from above, while Table 5b is the results of the Schneider dome area case. The results is used to demonstrate how normalization is performed

Table 5a. Schneider results (Albedo=29.4118, 1950) Table 5b. Schneider results (Albedo=29.3654%, 2019)

Surface	Albedo	% Area of Surface	Normalized Weighted Earth Area	Normalized Weighted Albedo %
	A	B	C=A x B x (1-0.67)	A x C
Sum of Water Type		71		
Sea Ice	0.6	15	4.95	2.970
Water	0.06	56	18.48	1.109
Sum of Land Type		29		
Land - (UHI + Coverage)	0.3118	28.941	9.55053	2.978
UHI + Coverage	0.12	0.059	0.01947	0.002
		Σ=100.000	33.000	7.05882
			Cloud Area	
Clouds	0.3336	67	67	22.35294
Σ Sum Earth %			100.000	
Σ Global Albedo				29.4118

Surface	Albedo	Normalized % Surface Area	Normalized Weighted Earth Area	Normalized Weighted Albedo %
	A	B	C=A x B x (1-0.67)	A x C
Sum of Water Type		70.239		
Sea Ice	0.6	14.839	4.897	2.938
Water	0.06	55.4	18.282	1.097
Sum of Land Type		29.761		
Land - (UHI + Coverage)	0.3118	28.631	9.448	2.946
UHI + Coverage	0.12	1.1307	0.373	0.0447757
		Σ=100.000	33.000	6.980769
			Cloud Area	
Clouds	0.3336	67	67	22.3530
Σ Sum Earth %			100.000	
Σ Global Albedo				29.3786

Normalization is done as follows:

1. Model starts with 1950 Table 5a albedo 29.4118%, then 2019 urban coverage area is entered.
2. For example, in Table B1, the new area increases from 0.059% to 1.143%. This is 1.084% larger, now the 'Sum of % of Earth Area' will be 101.521% in 2019.
3. All areas are renormalized to 101.084%. For example, sea ice at 15% in 1950 becomes 15%x(100.000/101.084)= 14.839% and the Urban Coverage becomes 1.143%x(100/101.521)=1.131%.

382 Appendix C: Related Warming Estimates and Other Amplification Factors

383

384 Although the results obtained here at first seem to indicate that UHIs do not appear to contribute much to global
 385 warming, when other factors are considered, much stronger significance can be estimated. In this appendix,
 386 additional feedback factors are suggested providing a number of global warming estimates.

387

- 388 • *Such factors can be contentious; however, it is not uncommon to look at how factors effect each other*
 389 *climate science. Therefore, we have chosen to provide these in this appendix mainly as an aid for the*
 390 *reader to illustrate how climate sensitivity can factor into the magnitude of UHIs warming significance.*
 391 *These estimates should be considered only as ballpark values.*

392

393 C.1 Global Feedback Amplification Factors

394

395 There is a wide range of possible estimates of climate feedback sensitivity driven by uncertainties in how water
 396 vapor, clouds, and other factors change as the Earth warms. Climate feedbacks are mixed and some will amplify
 397 (positive feedback) or diminish the effect of warming from the root cause effects (see for example Hausfather 2018).
 398 The actual feedback is known to be positive (van Nes, 2015). Climatologists will often approximate such factors
 399 frequently in reference with CO₂ doubling theory as positive. For example, water-vapor feedback alone, which is
 400 one of the most important in our climate system, is thought to have the capacity to about double the direct warming
 401 (Manabe and Wetherald, 1967; Randall et al., 2007, Dessler et. Al, 2008). This results from the fact that warm air
 402 holds more greenhouse moisture gas. Climate models incorporate this feedback. Water vapor feedback is strongly
 403 positive, with most evidence supporting a magnitude of 1.6 to 2.0 W/m²/K (Dessler et. al., 2008). Also water vapor
 404 feedback is considered a faster feedback mechanism (Hansen, 2008). We will use a factor of 1.75, a bit less than a
 405 doubling factor of 2. This factor would apply equally to UHI warming contribution, Greenhouse Gases (GHG), or
 406 warming due to sea ice melting.

407

408 C.2 WAASU Model Applied to the Melting of Sea Ice

409

410 While the Antarctic sea ice has remained roughly constant, the Arctic sea ice is melting at an alarming rate of
 411 12.85% in the last two decades (NASA sea ice, 2019). This apparent trend appears to yield about a 26% change in
 412 sea ice loss. It is difficult to find a strong reference for quantifying global warming impact due to Arctic sea ice
 413 melting. However, we might get a rough ballpark approximation using the WAASU model (and also illustrate one of
 414 the strengths of the model). Sea ice melting will results in a significant albedo change that roughly change in ice
 415 albedo of 0.6, to the open ocean albedo of 0.06 (see Table C1 and C2). Fortunately, the Arctic areas receive only
 416 about 40% as much solar radiation (Sciencing, 2018) reducing the feedback effect. From Equation 6, the effective
 417 sea ice surface area reduction from the irradiance decrease can be approximated as

418

$$419 \text{ Effective sea ice surface area} = 15\% (1 - 0.26 \times 0.40) = 13.44\% \text{ (a 1.56\% reduction of effective area).} \quad (\text{C-1})$$

420

421 In the WAASU model, we will have to make an assumption that the effective ocean surface area increases
 422 proportionately by 1.56% to 57.56% (see Table C2). The model then finds that the global albedo change decreases
 423 from 29.4118 to 28.9948%. (Note that alternately we could have set the albedo to 29.4118% in 2019 and worked
 424 back to 1950. In this case the albedo would have increase to 29.83%).

425

426 The Global Warming (GW) is found as:

$$427 \%GW = \{(P/\epsilon\sigma)^{0.25}_{2019} - (P/\epsilon\sigma)^{0.25}_{1950}\} / 0.95^\circ\text{C}, \quad (\text{C-2})$$

428

429 where $P = 340 \text{ W/m}^2 \times (1 - \text{Albedo})$ and $\epsilon = 1$. The warming increase due to ice melting is estimated from this model to
 430 be about 0.25°C or 26.4% of the 0.95°C increase in 2019. The increase in radiative forcing is 0.9452 W/m². The
 431 feedback is then roughly 1 W/m²/K where we assume a temperature change of 0.95C over this time period.

432

433 This estimate should only be taken as ballpark due to numerous uncertainties as climatologists find it hard to fully
 434 quantify the seasonal variations in ice change and to know the possible impact on cloud coverage increase from
 435 additional warming evaporation. However, one would expect less evaporation in the Arctic. Thus, there are a lot of
 436 uncertainties.

437 **Table C1.** Schneider results (Albedo=29.4118, 1950) **Table C2.** Sea ice loss - albedo change (29.0643%, 2019)

Surface	Albedo	% Area of Surface	Normalized Earth Area	Weighted Albedo %
	A	B	C=A x B x (1-0.67)	A x C
Sum of Water Type		71		
Sea Ice	0.6	15	4.95	2.970
Water	0.06	56	18.48	1.109
155Sum of Land Type		29		
Land - (UHI + Coverage)	0.3118	28.941	9.55053	2.978
UHI + Coverage	0.12	0.059	0.01947	0.002
		Σ=100.000	33.000	7.05882
			Cloud Area	
Clouds	0.3336	67	67	22.35294
Σ Sum Earth %			100.000	
Σ Global Albedo				29.4118

Surface	Albedo	Normalized % Surface Area	Normalized Earth Area	Weighted Albedo %
	A	B	C=A x B x (1-0.67)	A x C
Sum of Water Type		71		
Sea Ice	0.6	13.44	4.4352	2.507
Water	0.06	57.56	18.9948	1.14
Sum of Land Type		29	23.43	
Land - (UHI + Coverage)	0.3118	28.941	9.55053	2.978
UHI + Coverage	0.12	0.059	0.01947	0.002
		100.000	33.000	6.6395
			Cloud Area	
Clouds	0.3336	67	67	22.3530
Σ Sum Earth %			123.430	
Σ Global Albedo				29.1338

438
439 **C.3 Ballpark Contributions to Equilibrium Global Warming**

440
441 Table C3 summarizes the key global warming cause and effect factors that we have described.

442
443 **Table C3.** Global warming factors of interest

Urban Climate Amplification	Effects	Where Applied
UHI Area Amplification Factor	3.1 UHI Amplification	Applied to 2019 UHI Area
UHI Dome Horizontal Method	2.9 UHI Amplification	Applied to 2019 UHI Area
Ice Melting	0.25°C	25°C out of 0.95°C
Atmospheric Moisture Increase	1.75 GW Amplification	Applied to Ice Melting Temp, UHI, and GHGs +X*

444 where X is any other feedbacks (positive or negative)

445
446 Then major contributions to global warming can be simplified as follows for steady state warming

447
448
$$\Delta T_{GW} = \Delta T_{UHI} + \Delta T_{Water-Vapor} + \Delta T_{Sea-Ice} + \Delta T_{GHG} + \Delta T_X, \tag{C-3}$$

449
450 where $\Delta T_{GW}=0.95^\circ\text{C}$, $\Delta T_{UHI-Schneider}=0.011^\circ\text{C}$ (Table 7), $\Delta T_{Sea-Ice}=0.25^\circ\text{C}$, λ is the feedback, and ΔF is the radiative forcing change. We have three unknowns $\Delta T_{Water-Vapor}$, ΔT_{GHG} and ΔT_X . Here X is for all other feedback mechanisms like lapse rate and increases in cloud coverage and so forth, so this value can be both positive or negative. With one

451
452 assumption and the following two equations we can obtain some estimates:
453
454
455
$$0.95^\circ\text{C} = AF_{water\ vapor} (\Delta T_{UHI} + \Delta T_{GHG}) + \Delta T_X + \Delta T_{Sea-Ice} = 1.75 (0.0146^\circ\text{C} + \Delta T_{GHG}) + \Delta T_X + 0.25^\circ\text{C} \tag{C-4}$$

456 and
457
$$0.95^\circ\text{C} = \Delta T_{UHI} + \Delta T_{GHG+X} + \Delta T_{Sea-Ice} + \Delta T_{Water-Vapor} = 0.0147^\circ\text{C} + \Delta T_{GHG+X} + 0.25^\circ\text{C} + \Delta T_{Water-Vapor}. \tag{C-5}$$

458
459 At this point we need to make an assumption to obtain some example values. We will assume that $T_{GHG}=40\%$ of global warming so that $\Delta T_{GHG}=0.38^\circ\text{C}$. Using this estimate, with the water vapor $AF_{water-vapor}=1.75$ discussed above, and equation C-4 and C5, we obtain the examples in Table C3.

460
461
462 We note that in terms of root-causes, these examples illustrate how it is possible for the UHI effect (and coverage) contribution to global warming could range between 2.9 to 27%.

463
464
465 From the table the UHI effective feedback contribution are 2.43 (2.87%/1.18%), 2.3 (7.32%/3.16%), 2.2 (12.5%/5.7%), 1.8 (27.3%/15%) averaging 2.. This indicates that the UHI area feedback contribution could increase by 2.2 from 0.096 to about 0.21 W/m²/%Effective Normalized Area (see Table 7). Although these values are crude estimates, they serve as possible helpful examples.

473

Table C3. Global warming contributions (2019)

Warming Component	Temperature Contribution (°C)	% of GW Root Cause	Percent of GW	Temperature Contribution (°C)	% of GW Root Cause	Percent of GW
Schneider Study						
UHI Area Amplification=3.1			UHI Dome Amplification=8.4			
Urbanization	0.0112	2.87%	1.18%	0.03002	7.32%	3.16%
Greenhouse gases (40%)	0.38	97.13%	40.0%	0.38	92.68%	40.00%
Sea ice melting feedback	0.25		26.32%	0.25		26.32%
Water vapor feedback	0.2944		31%	0.31028		32.66%
X (Other)	0.0144		1.51%	-0.0203		-2.14%
Total	∑0.95					
GRUMP Study						
UHI Area Amplification=3.1			UHI Dome Amplification=8.4			
Urbanization	0.0542	12.47%	5.70%	0.1425	27.27%	15.00%
Greenhouse gases (35%)	0.38	87.53%	40%	0.38	72.73%	40.00%
Sea ice melting feedback	0.25		26.32%	0.25		26.32%
Water vapor feedback	0.331		34.8%	0.405		42.63%
X (Other)	-0.0648		-6.82%	-0.2275		-23.95%
Total	∑0.95					

474

475 **Appendix D: WAASU Model References**

476

477 Table D1 provides references for the WAASU model values.

478

479

Table D1 Key References for WAASU model

Parameter	Albedo (reference)	1950 Area (reference)
Sea Ice	50-70%, average 60% (NSID 2020)	15% (Lindsey 2019)
Water	0.06 (NSIDC 2020)	56% Ocean+Sea Ice=71% (USGS)
Land-(UHI+Coverage)	Adjusted to obtain 29.412% and surface reflected of 7.06 Earth Albedo in 1950 thereafter held fixed (see IPCC Hartmann (2013) AR5 report)	29%-Urban Coverage
UHI+Cov	0.12 Sugawara et. Al (2014)	See Table 1
Clouds	22.35294 (IPCC Hartmann et al., 2013)	67% (Earthobservatory, NASA)
Earth Albedo	29.412% (IPCC Hartmann, 2013)	-

480

481 **References**

482

483 Barr J. M., 2019 The Economics of Skyscraper Height (Part IV): Construction Costs Around the World, <https://buildingtheskyline.org/skyscraper-height-iv/>

484 Basara J. ,P. Hall Jr. , A.Schroeder , B.Illston ,K.Nemunaitis 2008, Diurnal cycle of the Oklahoma City urban heat island, J. of Geophysical Research

485 Cao C.X. , Zhao J., P. Gong, G. R. MA, D.M. Bao, K.Tian, Wetland changes and droughts in southwestern China, Geomatics, Natural Hazards and Risk, Oct 2011,

486 <https://www.tandfonline.com/doi/full/10.1080/19475705.2011.588253>

487 Cormack L. 2015 Where does all the stormwater go after the Sydney weather clears? The Sydney Morning Herald,

488 <https://www.smh.com.au/environment/where-does-all-the-stormwater-go-after-the-sydney-weather-clears-20150430-1mx4ep.html>489 Dessler A. E. ,Zhang Z., Yang P., Water-vapor climate feedback inferred from climate fluctuations, 2003–2008, *Geophysical Research Letters*, (2008), <https://doi.org/10.1029/2008GL035333>490 Earthobservatory, NASA (clouds albedo 0.67) <https://earthobservatory.nasa.gov/images/85843/cloudy-earth>491 Fan, Y., Li, Y., Bejan, A. *et al.* Horizontal extent of the urban heat dome flow. *Sci Rep* 7, 11681 (2017). <https://doi.org/10.1038/s41598-017-09917-4>492 Feddema, J. J., K. W. Oleson, G. B. Bonan, L. O. Mearns, L. E. Buja, G. A. Meehl, and W. M. Washington (2005), The importance of land-cover change in simulating future climates, *Science*, **310**, 1674– 1678, doi:10.1126/science.1118160493 Galka M. 2016, Half the World Lives on 1% of Its Land, Mapped, <https://www.citylab.com/equity/2016/01/half-earth-world-population-land-map/422748/>, (2016 publication on 2000 data set, <http://metrocosm.com/world-population-split-in-half-map/>)

503

- 504 Global Rural Urban Mapping Project (GRUMP) 2005, Columbia University Socioeconomic Data and Applications
505 Center, Gridded Population of the World and the Global Rural-Urban Mapping Project (GRUMP).
- 506 Hansen, J., "2008: Tipping point: Perspective of a climatologist." Archived 2011-10-22 at the Wayback Machine,
507 Wildlife Conservation Society/Island Press, 2008. Retrieved 2010.
- 508 Hartmann, D.L., A.M.G. Klein Tank, M. Rusticucci, L.V. Alexander, S. Brönnimann, Y. Charabi, F.J. Dentener,
509 E.J. Dlugokencky, D.R. Easterling, A. Kaplan, B.J. Soden, P.W. Thorne, M. Wild and P.M. Zhai, 2013:
510 Observations: Atmosphere and Surface. In: Climate Change 2013: The Physical Science Basis. Contribution of
511 Working Group I to the Fifth Assessment Report of the Intergovernmental Panel on Climate Change [Stocker,
512 T.F., D. Qin, G.-K. Plattner, M. Tignor, S.K. Allen, J. Boschung, A. Nauels, Y. Xia, V. Bex and P.M. Midgley
513 (eds.)]. Cambridge University Press, Cambridge, United Kingdom and New York, NY, USA.
- 514 Hirshi M. ,Seneviratne S. , V. Alexandrov, F. Boberg, C. Boroneant, O. Christensen, H. Formayer, B. Orlowsky &
515 P. Stepanek, Observational evidence for soil-moisture impact on hot extremes in Europe, *Nature Geoscience* 4,
516 17-21 (2011)
- 517 Huang Q. , Lu Y. 2015 Effect of Urban Heat Island on Climate Warming in the Yangtze River Delta Urban
518 Agglomeration in China, *Intern. J. of Environmental Research and Public Health* 12 (8): 8773 (30%)
- 519 Jones, P. D., D. H. Lister, and Q.-X. Li, 2008: Urbanization effects in large-scale temperature records, with an
520 emphasis on China. *J. Geophys. Res.*, 113, D16122, doi: 10.1029/2008JD009916.
- 521 Lindsey R, Scott M., (2019), Climate Change: Arctic Sea Ice Summer Minimum, NOAA Climate.gov,
522 <https://www.climate.gov/news-features/understanding-climate/climate-change-minimum-arctic-sea-ice-extent>
- 523 Manabe, S., and R. T. Wetherald (1967), Thermal equilibrium of atmosphere with a given distribution of relative
524 humidity, *J. Atmos. Sci.*, 24, 241–259.
- 525 McKittrick R. and Michaels J. 2004. A Test of Corrections for Extraneous Signals in Gridded Surface Temperature
526 Data, *Climate Research*
- 527 McKittrick R., Michaels P. 2007 Quantifying the influence of anthropogenic surface processes and inhomogeneities
528 on gridded global climate data, *J. of Geophysical Research-Atmospheres*
- 529 McKittrick Website Describing controversy: <https://www.rossmckittrick.com/temperature-data-quality.html>
- 530 NASA 1900-2006 updated, 2020 <https://climate.nasa.gov/vital-signs/global-temperature/>
- 531 NASA 2000, Gridded population of the world, , [https://sedac.ciesin.columbia.edu/data/set/gpw-v3-population-](https://sedac.ciesin.columbia.edu/data/set/gpw-v3-population-count/data-download)
532 [count/data-download](https://sedac.ciesin.columbia.edu/data/set/gpw-v3-population-count/data-download)
- 533 NASA Sea Ice, (2019) <https://climate.nasa.gov/vital-signs/arctic-sea-ice/>
- 534 NSID 2020, National Snow & Ice Data Center, "Thermodynamics: Albedo". nsidc.org. Retrieved 14 August 2016.
535 <https://nsidc.org/cryosphere/seaice/processes/albedo.html>
- 536 Randall, D. A. et al. (2007), Climate models and their evaluation, in *Climate Change 2007: The Physical Science*
537 *Basis. Contributions of Working Group I to the Fourth Assessment Report of the Intergovernmental Panel on*
538 *Climate Change*, edited by S. Solomon et al., pp. 591–662, Cambridge Univ. Press, Cambridge, U.K.
- 539 Ren, G.; Chu, Z.; Chen, Z.; Ren, Y. 2007 Implications of temporal change in urban heat island intensity observed at
540 Beijing and Wuhan stations. *Geophys. Res. Lett.* , 34, L05711,doi:10.1029/2006GL027927.
- 541 Ren, G.-Y., Z.-Y. Chu, J.-X. Zhou, et al., (2008): Urbanization effects on observed surface air temperature in North
542 China. *J. Climate*, 21, 1333-1348
- 543 Schmidt G. A. 2009 Spurious correlations between recent warming and indices of local economic activity, *Int. J. of*
544 *Climatology*
- 545 Schneider, A., M. Friedl, and D. Potere, 2009: A new map of global urban extent from MODIS satellite data.
546 *Environmental Research Letters*, 4(4), 044003, doi:10.1088/1748-9326/4/4/044003
- 547 Satterthwaite D.E., F. Aragón-Durand, J. Corfee-Morlot, R.B.R. Kiunsi, M. Pelling, D.C. Roberts, and W. Solecki,
548 2014: Urban areas. In: *Climate Change 2014: Impacts, Adaptation, and Vulnerability. Part A: Global and*
549 *Sectoral Aspects. Contribution of Working Group II to the Fifth Assessment Report of the Intergovernmental*
550 *Panel on Climate Change (IPCC)*
- 551 Sciencing (2018) <https://sciencing.com/sun-intensity-vs-angle-23529.html>
- 552 Stone B. 2009 Land use as climate change mitigation, *Environ. Sci. Technol.*, 43(24), 9052– 9056,
553 doi:10.1021/es902150g
- 554 Sugawara, H., Takamura, T. Surface Albedo in Cities (0.12): Case Study in Sapporo and Tokyo, Japan. *Boundary-*
555 *Layer Meteorol* **153**, 539–553 (2014). <https://doi.org/10.1007/s10546-014-9952-0>
- 556 US Population Growth 1900-2006, u-s-history.com/pages/h980.html
- 557 USGS 1900-2006, Materials in Use in U.S. Interstate Highways, <https://pubs.usgs.gov/fs/2006/3127/2006-3127.pdf>
- 558 USGS on Amount of Earth covered by water, [https://www.usgs.gov/special-topic/water-science-](https://www.usgs.gov/special-topic/water-science-school/science/how-much-water-there-earth?qt-science_center_objects=0#qt-science_center_objects)
559 [school/science/how-much-water-there-earth?qt-science_center_objects=0#qt-science_center_objects](https://www.usgs.gov/special-topic/water-science-school/science/how-much-water-there-earth?qt-science_center_objects=0#qt-science_center_objects)
- 560 van Nes E. H., Scheffer M., Brovkin V., Lenton T. M., Ye H, Deyle E. and Sugihara G., *Nature Climate Change*
561 2015. [dx.doi.org/10.1038/nclimate2568](https://doi.org/10.1038/nclimate2568)
- 562 World Bank, 2018 population growth rate, worldbank.org
- 563 Yang, X.; Hou, Y.; Chen, B. 2011 Observed surface warming induced by urbanization in east China. *J. Geophys.*
564 *Res. Atmos*, 116, doi:10.1029/2010JD015452.

- 565 Zhang, X., Friedl, M. A., Schaaf, C. B., Strahler, A. H. & Schneider, A. 2004 The footprint of urban climates on
566 vegetation phenology. *Geophys. Res. Lett.* 31, L12209
- 567 Zhao, Z.-C., 1991: Temperature change in China for the last 39 years and urban effects. *Meteorological Monthly* (in
568 Chinese), 17(4), 14-17.
- 569 Zhao, Z.-C., 2011: Impacts of urbanization on climate change. in: 10,000 Scientific Difficult Problems: Earth
570 Science, 10,000 scientific difficult problems Earth Science Committee Eds., Science Press, 843-846. 30%
- 571 Zhao L, Lee X, Smith RB, Oleson K, Strong 2014, contributions of local background climate to urban heat islands,
572 *Nature*. 10;511(7508):216-9. doi: 10.1038/nature13462
- 573 Zhou D. , Zhao S. , L. Zhang, G Sun and Y. Liu, 2015, The footprint of urban heat island effect in China, *Scientific*
574 *Reports*. 5: 11160
- 575 Zhou Y. , SmithS. , Zhao K. , M. Imhoff, A. Thomson, B. Lamberty,G. Asrar, X. Zhang, C. He and C. Elvidge, A
576 global map of urban extent from nightlights, *Env. Research Letters*, 10 (2015), (study uses a 2000 data set).
- 577
- 578
- 579

580 **Conflicts of Interest**

581 The author declares that he has no conflicts of interest.

582

583

1.